Polymer 51 (2010) 3948–3955

Contents lists available at ScienceDirect

Polymer

journal homepage: www.elsevier.com/locate/polymer

Synthesis and characterization of polyhedral oligomeric silsesquioxane (POSS) with multifunctional benzoxazine groups through click chemistry

Yi-Chen Wu, Shiao-Wei Kuo*

Department of Materials and Optoelectronic Science, Center for Nanoscience and Nanotechnology, National Sun Yat-Sen University, Kaohsiung 804, Taiwan

ARTICLE INFO

Article history:
Received 28 January 2010
Received in revised form
3 June 2010
Accepted 22 June 2010
Available online 1 July 2010

Keywords:
POSS
Click chemistry
Polybenzoxazine

ABSTRACT

We prepared a new class of polybenzoxazine-POSS nanocomposites with network structures through thermal curing of multifunctional benzoxazine groups of POSS (OBZ-POSS), which was synthesized from octa-azido functionalized POSS ($OVBN_3$-POSS) with 3,4-dihydro-3-(prop-2-ynyl)-2*H*-benzoxazine (P-pa) via a click reaction. Incorporation of the silsesquioxane core into the polybenzoxazine matrix could significantly enhance the thermal stability of these hybrid materials. For these nanocomposites, the POSS nanoparticles in the hybrids were improved their thermal properties with 2,2-bis(3,4-dihydro-3-methyl-2*H*-1,3-benzoxazine)propane (BA-m) and P-pa polybenzoxazine, analyzed via TGA analyses. In addition, the incorporation of the POSS led to the formation of an inorganic protective layer on the nanocomposite's surface. Contact angle data provided positive evidence to back up this hypothesis that the incorporation of the POSS units would decrease the surface energy property. In addition, the low glass transition temperature of poly(4-vinyl pyridine) and polycarbonate thin films, which lack liquid resistance, could possess low surface free energy after modification with OBZ-POSS due to low temperature curing of this new compound.

1. Introduction

Benzoxazines are heterocyclic compounds generated by the Mannich condensation of phenol, formaldehyde, and primary amine [1,2]. They can be polymerized via a thermally induced ring-opening polymerization without using strong acid or base as catalyst and thus no toxic gas or other byproducts is generated during polymerization. Near zero shrinkage upon polymerization, low water absorption, and high char yield are some of many advantages of benzoxazine resins [3,4]. Furthermore, polybenzoxazines (PBZ) have unique properties not found in traditional phenolic resins, such as excellent dimensional stability, flame retardance, stable dielectric constants, and low surface free energy [5–10].

To further improve the performance of polybenzoxazines, blending with other polymers [11–21] such as polyurethane and epoxy resin or organic–inorganic hybrid systems such as clay [21–23] and poly(imide-siloxane) [16] have been successfully allowed for benzoxazine resin modification. In addition, polymerizable acetylene and allyl side groups have been introduced to the benzoxazine monomers [24–30]. The acetylene and allyl functional benzoxazine can be polymerized into three dimensional network products that show improved high thermal and mechanical stabilities and high solvent and moisture resistances. Other elegant methods such as macromonomer formation, polymer modification, and "click chemistry" allow for combinations of benzoxazine structures with conventional polymers. During the last several years, click chemistry has become very popular for designing a variety of molecular architectures. In particular, the copper-catalyzed 1,3-dipolar cycloaddition of azides and alkynes has been intensively studied due to the number of obvious advantages [31–33]. Recently, researchers have reported polystyrene functionalized with benzoxazine by utilizing the click reaction as a new method for thermally curable polystyrene thermosets [34]. The presence of a thermally stable and corrosion-inhibiting triazole ring in the polymer backbone imparts additional favorable characteristics to polybenzoxazine. Ishida et al. also reported that linear benzoxazine containing polymers was synthesized via a click reaction [35]. More interestingly, the nature of the low temperature exotherm DSC peak (ca. 150 °C) was due to the thermal coupling of the residual propargyl and azide end group in the absence of active catalyst. In general, the requirement of high temperature curing (ca. 180–210 °C) of polybenzoxazine limits its broader application, especially for most polymer substrates. A method of lower temperature curing of benzoxazine is thus urgently needed to broaden the applications of PBZ with temperature sensitive substrates (T_g < curing temperature of PBZ) such as most polymeric materials [25,30,36,37].

* Corresponding author. Tel.: +886 7 5252000x4079; fax: +886 7 5254099.
E-mail address: kuosw@faculty.nsysu.edu.tw (S.-W. Kuo).

0032-3861/$ – see front matter © 2010 Elsevier Ltd. All rights reserved.
doi:10.1016/j.polymer.2010.06.033

Polymer-inorganic nanocomposites with improved properties have attracted extensive research interest during the past few years. If both components are mixed at the nanometer level, they usually exhibit improved performance properties compared to conventional composites. Recently, researchers have developed a novel class of organic/inorganic hybrid materials based on polyhedral oligomeric silsesquioxane (POSS) [38–47]. POSS is an inorganic Si_8O_{12} core, and the core can be functionalized by attaching seven inert organic hydrocarbon groups and a unique functional group or eight functional groups that are capable of polymerization or cross-linking [48–54]. If these inorganic POSS particles are evenly distributed within the organic matrix at the nanometer scale (1–100 nm), they can dramatically improve their thermal stabilities and mechanical strengths [55–57]. The POSS-containing polymers generally possess improved thermal stabilities, mechanical properties, surface hardening and have attracted considerable interest in versatile applications. In contrast to clay and conventional fillers, POSS particles have the advantages of possessing monodisperse molecular weights with well defined structures, lower densities, high and temperature stabilities while containing no trace metals. They also exhibit sizable interfacial interactions between the composite particles and polymer segments. Each POSS compound may contain one or more reactive sites; therefore, they can be easily incorporated into common polymers. To improve the property of the material, the POSS cage can be introduced into the matrix with polymerizable groups through a click reaction [58–60].

In this work, we synthesized POSS nanocomposites with benzoxazine groups through click reactions to enhance the thermal properties of polybenzoxazine. A multifunctional POSS bearing eight benzoxazine groups (OBZ-POSS) was synthesized through octa-azide POSS (OVBN3-POSS) and 3,4-dihydro-3-(prop-2-ynyl)-2*H*-benzooxazine (P-pa) via a click reaction. These polybenzoxazine-POSS hybrid materials resulted in noticeable thermal stability improvement, confirmed by TGA analyses. In this context, we found that OBZ-POSS could be cured at a relatively low temperature (120 °C) with lower surface energy [36]. Many polymer substrates, such as poly(4-vinyl pyridine) and similar polymers, could be coated by the modified polybenzoxazine in order to possess low surface energy.

2. Experimental section

2.1. Materials

Paraformaldehyde, and propargylamine were purchased from Tokyo Kasei Kogyo Co., Japan. Vinyl benzyl chloride (VBC), sodium azide (NaN_3), copper(I) bromide (CuBr, 98%), *N*,*N*,*N*′,*N*′′,*N*′′-penta methyldiethylenetriamine (PMDETA, 99%), and Platinum complex (platinum-1,3-divinyltetramethyldisiloxane, Pt-dvs, 2 wt% Pt in xylene) were purchased from Aldrich, USA. Before use, the solution of the platinum complex was diluted 100-fold with xylene. Toluene was dried by distillation before use in the hydrosilylation reaction. Octakis(dimethylsiloxy)silsesquioxane ($Q_8M_8^H$) containing eight hydro-silane groups was purchased from the Hybrid Plastics Co., USA. The benzoxazine monomer, 2,2-Bis(3,4-dihydro-3-methyl-2*H*-1,3-benzoxazine)propane (BA-m benzoxazine) was prepared according to the previous studies [61,62].

2.2. Preparation of 3,4-dihydro-3-(prop-2-ynyl)-2H-benzooxazine monomer (P-pa)

P-pa was synthesized through the procedure according to Scheme 1. Phenol (0.036 mol, 3.418 g), and propargylamine (0.018 mol, 1 g) were dissolved in dioxane in a 100-ml three necked flask and then paraformaldehyde (0.072 mol, 2.18 g) was added at room temperature. The solution was refluxed at 110 °C for 12 h. The crude product was dissolved in ether and washed several times with 3 N sodium hydroxide solution and finally with distilled water. Then, the ether solution was dried over sodium sulfate anhydrous, followed by evaporation of solvent under vacuum to afford pale yellow viscous fluid.

2.3. Synthesis of OVBC-POSS

OVBC-POSS was prepared via $Q_8M_8^H$ (1 g, 0.98 mmol) and vinyl benzyl chloride (1.20 g, 7.86 mmol) in toluene (50 mL). The solution was heated at 60 °C under argon and Pt(dvs) (0.07 mL, 0.13 mmol) was added via syringe. After stirring for 4 h, removal of the Pt(dvs) catalyst was through activated charcoal. The solvent in a rotary evaporator gave a viscous liquid.

2.4. Synthesis of $OVBN_3$-POSS

$OVBN_3$-POSS was synthesized via the reaction between OVBC-POSS and sodium azide (NaN_3). In a typical experiment, OVBC-POSS (1 g, 0.45 mmol), NaN_3 (1.01 g, 15.4 mmol) and anhydrous DMF (50 mL) were added to a flask. The reaction was thermostated at 120 °C for 48 h. The solvents were concentrated and the residues were dissolved in THF removal of the sodium salts through a neutral alumina column. The yellowish viscous liquid was obtained after drying in a vacuum oven overnight at room temperature.

2.5. Synthesis of OBZ-POSS through click reaction

$OVBN_3$-POSS (1 g, 0.44 mmol), P-pa (0.661 g, 3.821 mmol) and CuBr (3.5 mg, 0.025 mmol) were dissolved in DMF (20 mL) in a flask equipped with magnetic stirring bar. After one brief freeze-thaw-pump cycle, PMDETA (5.2 μL, 0.025 mmol) was added and the reaction mixture was carefully degassed by three freeze-thaw-pump cycles, placed in an oil bath thermostated at 60 °C and stirred for 24 h. After removing all the solvents at reduced pressure, the residues were dissolved in CH_2Cl_2 and passed through a neutral alumina column to remove copper catalysts. A dark brown viscous liquid was obtained. All chemical reactions of synthesizing OBZ-POSS were summarized in Scheme 2.

2.6. Preparation of polybenzoxazine/POSS nanocomposites

OBZ-POSS was stirred for 2 h at room temperature and tipped out on the aluminum plate for 6 h in open air to dry and placed in an oven at 100 °C under vacuum for 2 h. The cast film was polymerized in a stepwise manner, at 140 and 160 °C for 3 h each and then at 200 °C for 4 h. The product was postcured at 220 and 240 °C for 30 min each. All the cured samples were transparent with dark red color (ca. 0.2 cm thickness).

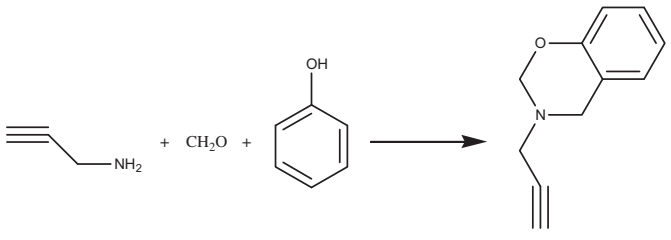

Scheme 1. Synthesis of P-pa.

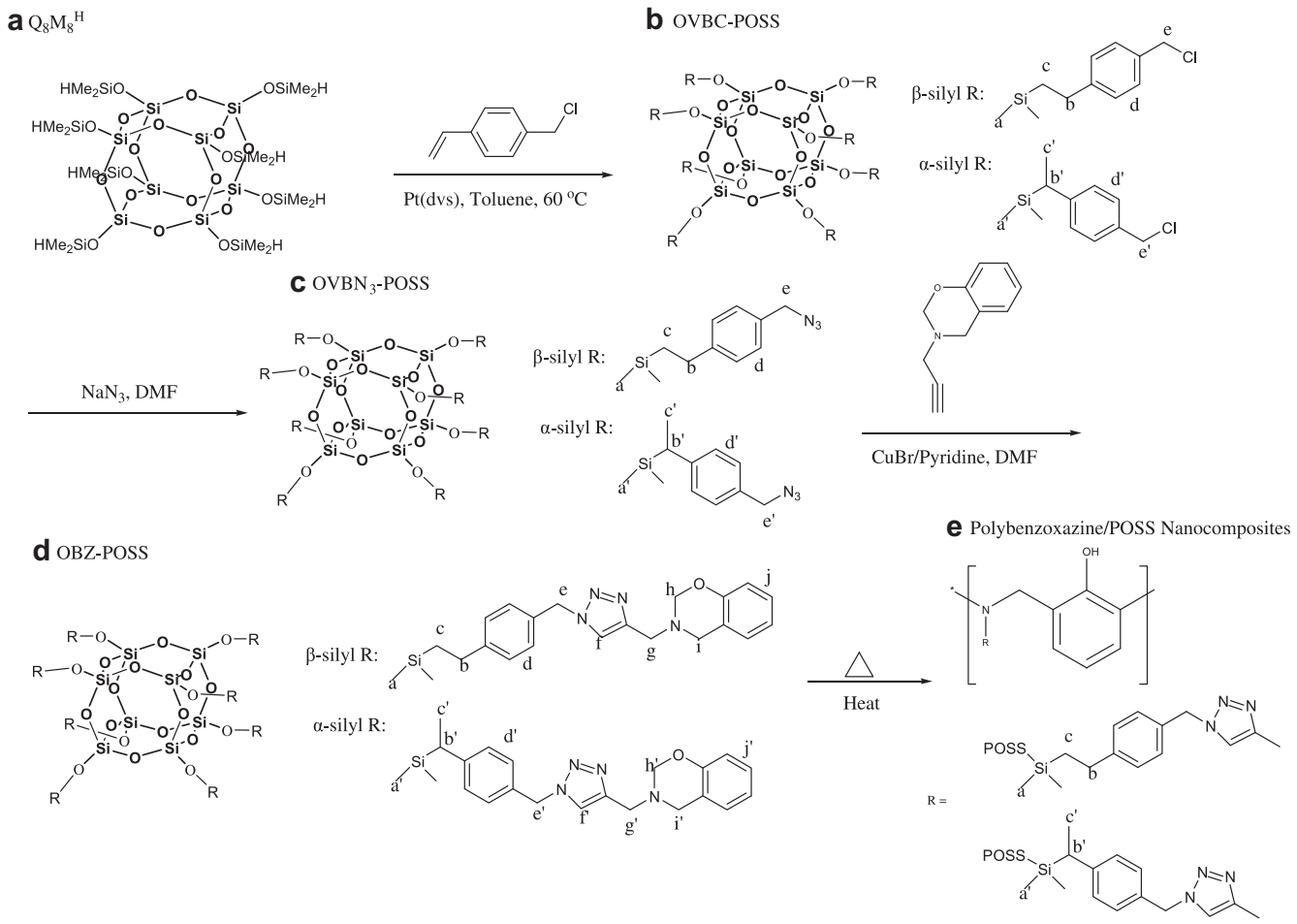

Scheme 2. Hydrosilylation of styrenic monomers with $Q_8M_8^H$ (a) to give OVBC-POSS (b) and $OVBN_3$-POSS (c) and click reaction to form OBZ-POSS (d) and thermal curing to form polybenzoxazine/POSS nanocomposites (e).

2.7. Characterizations

^{1}H nuclear magnetic resonance (NMR) spectra were obtained using an INOVA 500 instrument with $CDCl_3$ as solvent and TMS as the external standard. The value of the recycle delay is 2 s to ensure higher than $5T_1$(H) (spin-lattice relaxation time in the laboratory frame). Chemical shifts are reported in parts per million. FTIR spectra of the polymer blend films were recorded using the conventional KBr disk method. The films used in this study were sufficiently thin to obey the Beer–Lambert law. FTIR spectra were recorded using a Bruker Tensor 27 FTIR spectrophotometer; 32 scans were collected at a spectral resolution of 1 cm^{-1}. Because polymers containing hydroxyl groups are hygroscopic, pure N_2 gas was used to purge the spectrometer's optical box to maintain sample films dried. The dynamic curing kinetics was studied using a TA Q-20 Differential Scanning Calorimeter operating under a nitrogen atmosphere. The sample of (ca. 7 mg) was placed in a sealed aluminum sample pan. Dynamic curing scans were conducted from 30 °C to 350 °C at a heating rate of 10 °C/min. The thermal stability of the samples was characterized by using a TA Q-50 Thermogravimetric Analyzer operating under a nitrogen atmosphere. The cured sample ca. 7 mg was placed in a Pt cell and heated at a rate of 20 °C/min from 30 to 800 °C at a nitrogen flow rate of 60 mL/min. The thin film of OBZ-POSS was dissolved in tetrahydrofuran (THF) at room temperature. The solution was then filtered through a 0.2 mm syringe filter and spin coated onto a poly(4-vinyl pyridine) thin film on glass slide. The sample was then left to dry at 120 °C for 24 h to remove residual solvent for contact angle measurement. A Krüss GH-100 goniometer interfaced to image-capture software was used to measure the advancing contact angles of the samples at 25 °C; a liquid drop of deionized water, diiodomethane, and ethylene glycol (5 μL) was injected onto the polymer surface.

3. Results and discussion

3.1. Synthesis of P-pa

Fig. 1 displays the FTIR and ^{1}H NMR spectra of P-pa. Clearly, Fig. 1 (a) shows the acetylene ≡C–H and C≡C stretching vibration at 3290 cm^{-1} and 2121 cm^{-1}, respectively [28], and the carbon–carbon stretching vibration derived from the 1,2,4-substitution of the benzene ring of the P-pa appears at 1490 cm^{-1} and the asymmetric stretching of C–O–C at 1230 cm^{-1}. The ^{1}H NMR spectrum of P-pa (see Fig. 1(b)) shows the peaks at 3.6 and 4.9 ppm, corresponding to protons in the methylene bridge of the oxazine, and the singlet at 2.30 and 4.11 ppm, which correspond to ≡C–H and =CH_2 (propargyl), respectively, and the aromatic protons appeared as multiplets at 6.77–7.40 ppm.

3.2. Synthesis of $OVBN_3$-POSS

The peaks for the vinyl (ca. 5.3, 5.8, and 6.7 ppm) in Fig. 2(a) and Si–H protons (4.7 ppm) in Fig. 2(b) disappeared in the spectrum of OVBC-POSS, supporting the complete reaction of hydrosilylation.

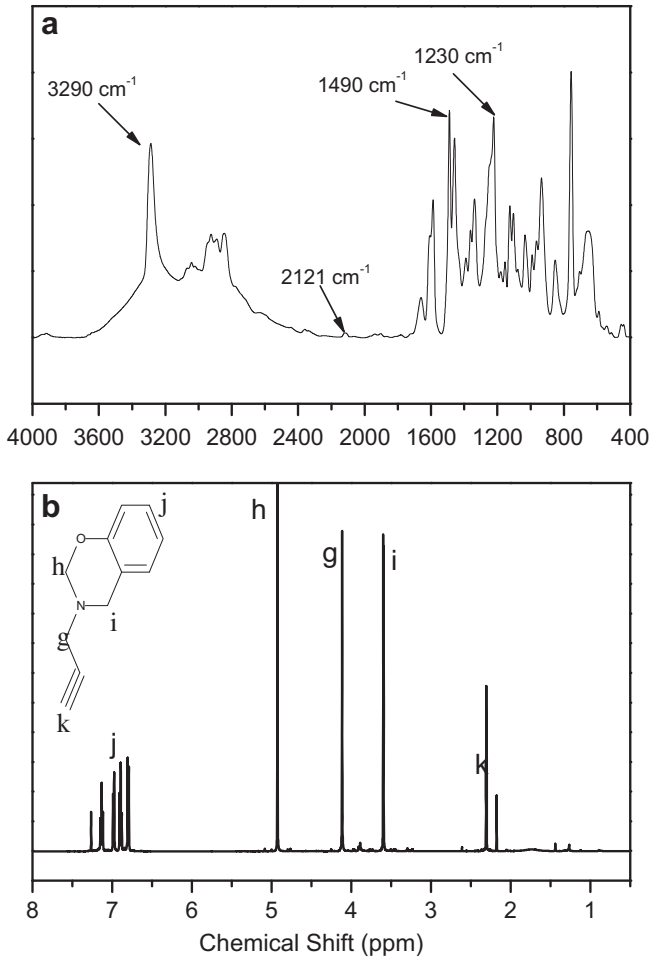

Fig. 1. (a) IR and (b) ^{1}H NMR spectra of P-pa in $CDCl_3$.

The spectrum in Fig. 2(c) indicates that the vinyl groups of VBC underwent hydrosilylation of the Si–H bonds of $Q_8M_8^H$ in both the α and β configurations, i.e., a mixture of these two orientations exists. We observed the ratios of β to α linkages (1.64:1) for OVBC-POSS, according to the integration of the signals for the protons on the benzylic carbon atoms marked *b* (2H, β-side groups) and *b*′ (1H, α-side groups), benzyl CH_2 (**H**$_e$) at $\delta = 4.50$ ppm, and the aromatic protons multiplet at 6.90–7.20 ppm, indicating the successful synthesis of OVBC-POSS. The complete substitution of chloride atoms by azido groups was confirmed by the ^{1}H NMR spectrum in Fig. 2(d). With the occurrence of the substitution reaction, the resonance of the benzyl CH_2 connected to the chloride atoms shifted to higher field – from 4.50 to 4.31 ppm [62]. The observation that no remnant resonance existed at 4.50 ppm suggested that the substitution reaction occurred to completion under the reaction conditions.

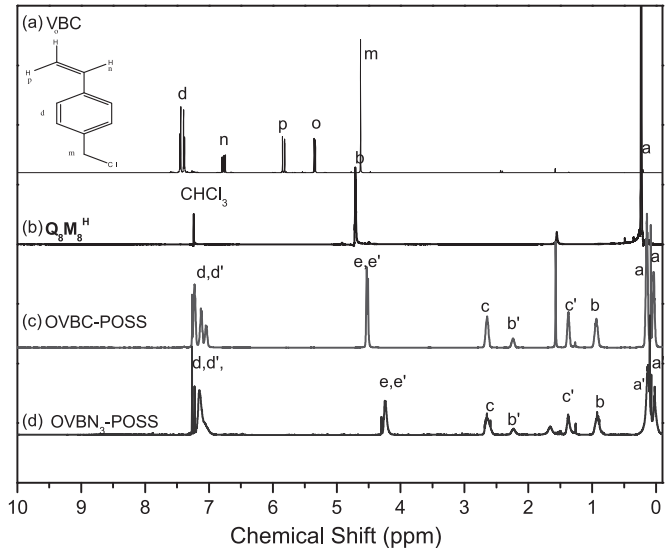

Fig. 2. ^{1}H NMR spectra of (a) VBC, (b) $Q_8M_8^H$, (c) OVBC-POSS, and (d) $OVBN_3$-POSS in $CDCl_3$.

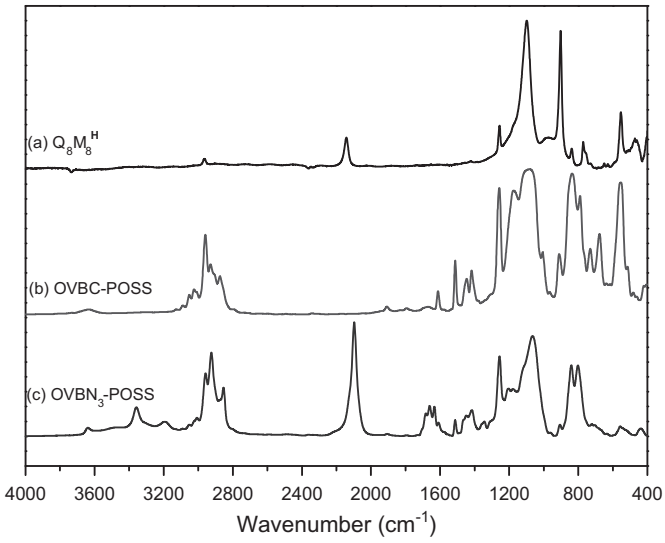

Fig. 3. FTIR spectra of (a) $Q_8M_8^H$, (b) OVBC-POSS, and (c) $OVBN_3$-POSS.

Fig. 3 presents the FTIR spectra of $Q_8M_8^H$, OVBC-POSS, and $OVBN_3$-POSS. The strong absorption peak around 1100 cm^{-1} for all compounds represented the vibrations of the siloxane Si–O–Si groups and is a general feature of POSS derivatives. The characteristic stretching vibrations of the Si–H group appeared as peak at 2200 cm^{-1} as shown in Fig. 3(a). In OVBC-POSS, this peak disappeared completely, indicating that reaction reached completion. The $OVBN_3$-POSS after the substitution reaction in Fig. 3(c) clearly

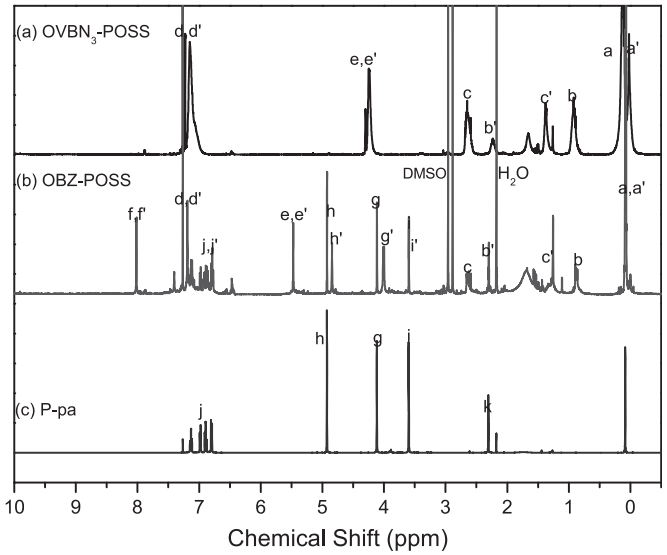

Fig. 4. ^{1}H NMR spectra of (a) $OVBN_3$-POSS, (b) OBZ-POSS and (c) P-pa in $CDCl_3$.

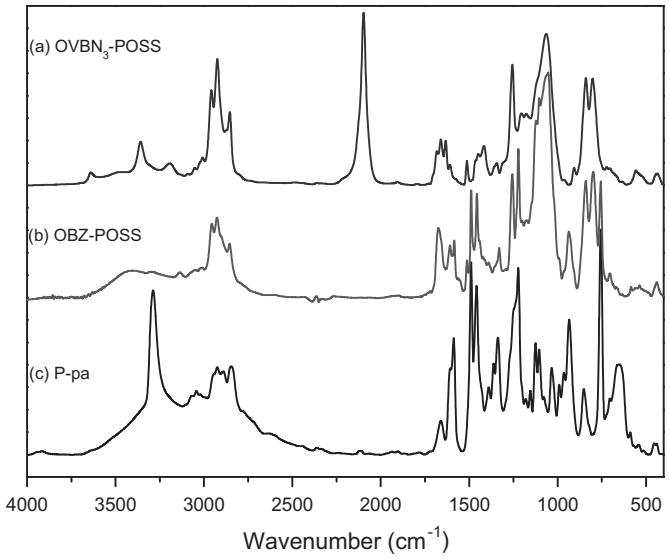

Fig. 5. FTIR spectra of (a) $OVBN_3$-POSS, (b) OBZ-POSS and (c) P-pa.

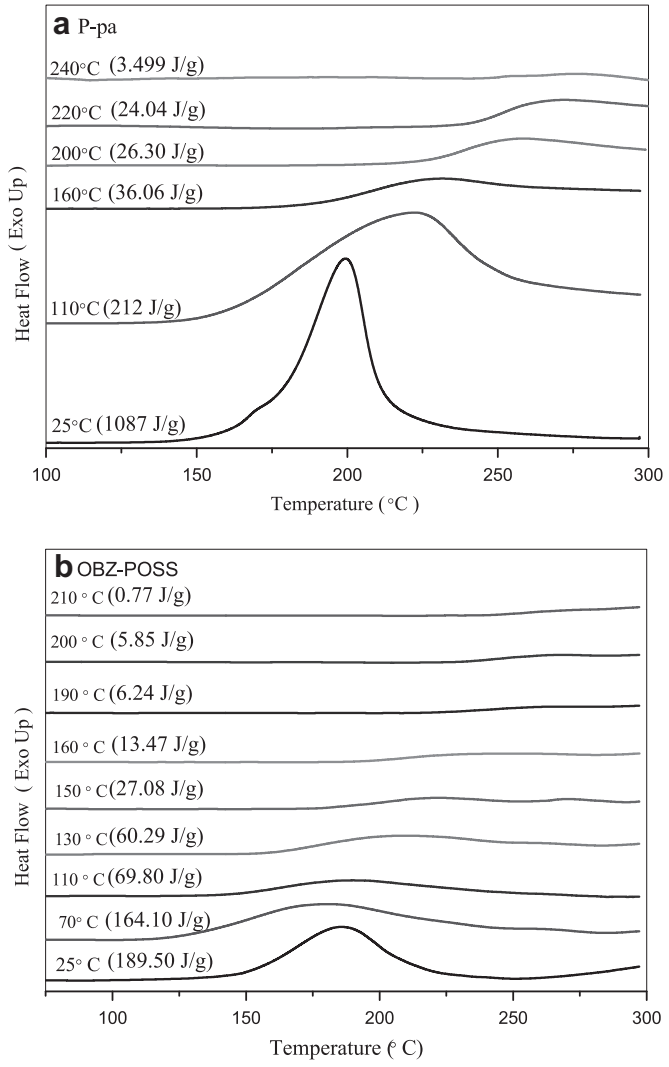

Fig. 6. DSC profile of (a) P-pa was cured at 110 °C for 3 h, at 160 and 200 °C for 2 h at 220 °C for 1 h and at 240 °C for 30 min (b) OBZ-POSS was cured at 70 °C for 3 h, at 110, 130 and 150 °C for 2 h, at 160 and 190 °C for 1 h, 200 and 210 °C for 30 min.

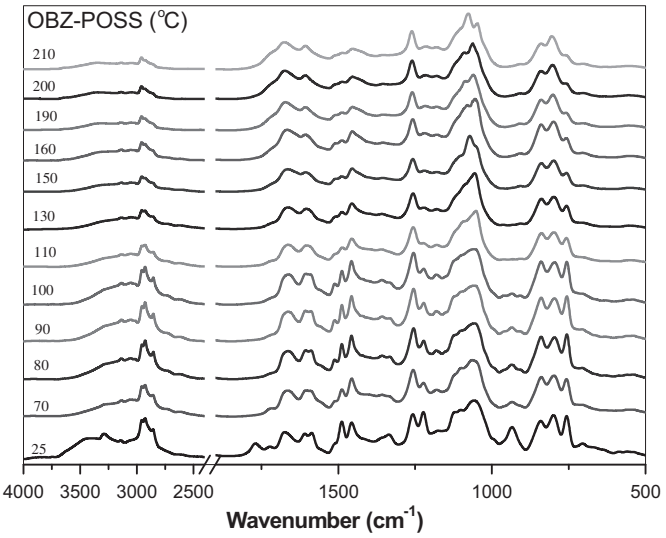

Fig. 7. FTIR spectra of OBZ-POSS after each cure stage.

showed the appeared peak at 2096 cm^{-1}, indicating the presence of the azido groups. All results based on ^1H NMR and FTIR analyses were indicative of the successfully synthesizing of $OVBN_3$-POSS.

3.3. Synthesis of OBZ-POSS

Fig. 4 shows the ^1H NMR spectra of OVBN3-POSS, P-pa, and OBZ-POSS. Compared to those of the two precursors, we could clearly observe the appearance of new signals at 8.0 ppm ($\mathbf{H}_f$) in the NMR spectrum of OBZ-POSS; the resonance at 8.0 ppm was due to the protons of the triazole structures resulting from the click reaction. In addition, the peaks at 3.6 and 4.9 ppm, corresponding to protons in the methylene bridge of the oxazine, and the peak at 4.11 ppm, corresponding to CH_2 (propargyl), remained in OBZ-POSS but split into two resonance peaks, indicating both α and β configurations in OBZ-POSS. In addition, the resonance of benzyl CH_2 connected to the azide atoms significantly shifted to down field – from 4.31 to 5.48 ppm. The observation that no remnant resonance existed at 4.31 ppm suggested that the click reaction occurred to completion under the reaction conditions.

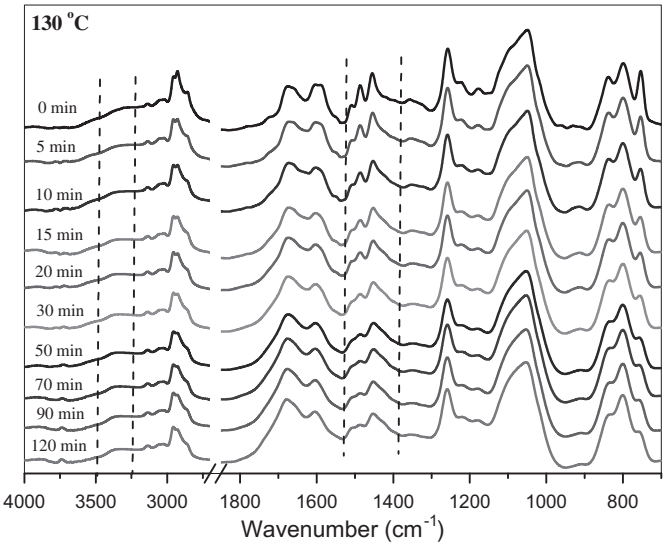

Fig. 8. FTIR spectra of OBZ-POSS after treatment at 130 °C for various curing times.

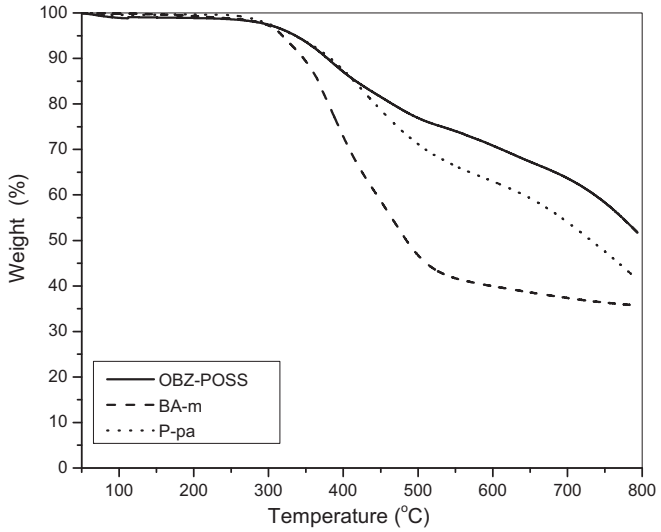

Fig. 9. TGA analyses of BA-m, P-pa and OBZ-POSS, after curing.

The complete disappearance of the characteristic azide and acetylene groups could also be confirmed by FTIR analysis as shown in Fig. 5. The peak at 2100 cm^{-1}, corresponding to the azide absorbance to $OVBN_3$-POSS, and 3290 cm^{-1}, corresponding to the acetylene group of P-pa was totally disappeared in OBZ-POSS, indicating that all the azide and acetylene functionalities participated in the click reaction. The remained trisubstituted aromatic ring of P-pa (1490 cm^{-1} and 943 cm^{-1}) in the benzoxazine structure and the Si–O–Si absorption (1100 cm^{-1}) of $OVBN_3$-POSS are shown in Fig. 5(b). All results based on ^1H NMR and FTIR analyses indicated that the synthesis of OBZ-POSS was successful.

3.4. Curing behavior of OBZ-POSS

We examined the curing behavior of P-pa and OBZ-POSS by DSC analyses. Fig. 6(A) shows the DSC profiles for the P-pa benzoxazine, which had an exotherm with a maximum at 200 °C. The amount of the exotherm reaction heat of P-pa was 1088 J/g Fig. 6(A) also shows the DSC profiles of P-pa after each cure cycle. The amount of the exotherm corresponding to the ring-opening of the oxazine ring and the cross-linking of the propargyl group decreased after each cure cycle and disappeared completely after the 240 °C cure. Fig. 6 (B) shows the DSC profiles for the OBZ-POSS with an exotherm peak at 180 °C with a heating rate of 10 °C/min. The total amount of the exotherm peak of OBZ-POSS was 190 J/g, which was smaller than pure P-pa due to the dilution effect of POSS which inhibited the thermal curing of the benzoxazine compound [3,27] and the loss of propargyl group of OBZ-POSS compared with P-pa. Fig. 6(B) also displays DSC curves of pure OBZ-POSS after each different thermal curing temperature. The amount of the exotherm peak decreased with the increase of the curing temperature and almost disappeared after the cure at 210 °C [27]. Interestingly, Ishida et al. reported a series of new benzoxazine polymers containing diacetylene groups in the main chain [30]. These polymers showed exothermic peaks exhibiting considerably lower cross-linking temperatures than those of conventional benzoxazines with a maximum at 185 °C. The results showed the lower temperature of the exothermic process related to the partial benzoxazine polymerization. In this study, the benzoxazine group with the triazole structure showed a lower exothermic peak at 180 °C compared with those of the benzoxazine polymers containing diacetylene groups by Ishida et al. In addition, Yagci et al. reported two exotherms with onsets around 150 °C and 250 °C of benzoxazine containing styrenic units with triazole structures with a 250 °C exotherm peak, corresponding to the ring-opening polymerization for the benzoxazine moiety, but for the low temperature exothermic peak, which was attributed to the rearrangement of the triazole ring [34]. Ishida et al. suggested that this phenomenon might be attributed to the contribution from the end groups of the polymers due to the thermal coupling of the residual propargyl and azide end groups of linear polymers containing benzoxazine and triazole moieties [35]. However, we observed only one exotherm of OBZ-POSS in this study, and the low exotherm peak shifted from 150 °C to 185 °C. To the best of our knowledge, there is no information about the thermal curing of this new compound.

To make clear which reaction is involved in the exotherm observed by DSC, we characterized the curing process of the pure OBZ-POSS systems by FTIR spectroscopy at different temperatures. Fig. 7 shows IR spectra after each cure cycle of pure OBZ-POSS. Clearly, the characteristic absorption band assigned to the unsaturations of the =C–H bonds in the triazole structures, indicated by peaks such as those at 3080 cm^{-1}, was maintained after thermal curing. The band representing the trisubstituted aromatic ring of OBZ-POSS (1490 cm^{-1} and 943 cm^{-1}) assigned to the trisubstituted aromatic ring in the benzoxazine structure in Fig. 7(a). The broad absorption band at 2500–3500 cm^{-1} in Fig. 7(b)–(g), assigned to the three different types of hydrogen bonding interactions, included the $O^-–H^+N$ intramolecular hydrogen bonding around 2750 cm^{-1}, the OH–N intramolecular hydrogen bonding around 3200 cm^{-1}, the OH–O intermolecular hydrogen bonding around 3420 cm^{-1}, all of which have been discussed in a previous study [63]. More importantly, the maximum peak position of the siloxane vibration band shifted from 1052 cm^{-1} for the uncured OBZ-POSS (see Fig. 4(a)) to 1076 cm^{-1} after thermal curing as shown in Fig. 7(b) and (g). These results indicated that the siloxane group of POSS might interact with the hydroxyl group of the polybenzoxazine. We believe that the interaction caused by the formation of the multi-hydrogen bonds between the POSS siloxane and the polybenzoxazine hydroxyl was responsible for the absorption shift of the siloxane vibration band [64]. In addition, the characteristic absorption band at 943 cm^{-1} due to the trisubstituted benzene ring was totally disappeared at 110 °C, which was significantly lower than the temperature typical of P-a (3-phenyl-3,4-dihydro-2*H*-1,3-benzoxazine), P-ala (3-allyl-3,4-dihydro-2*H*-1,3-benzoxazine), and P-appe (4-propargyloxyphenyl-3,4-dihydro-2***H***-1,3-benzoxazine) in which this peak disappeared around 200° C–240 °C [26–28]. As a result, the triazole structure of OBZ-POSS might act as a catalyst for the enhancement of the benzoxazine resin polymerization based on the FTIR analysis.

Table 1
Surface free energy, and thermal properties of BA-m, P-pa and OBZ-POSS systems.

Polymers	Roughness (nm)	Contact angle (o)			γ (mJ/m^2)	Thermal property		Thermal curing	
		H_2O	DIM	EG		T_d (°C)	Char (wt%) (790 °C)	T_p (°C)	ΔH_{curing} (J/g)
BA-m	7.8	105.5	79.8	77.5	18.6	380.1	36.8	213.3	346.9
P-pa	20.4	110.0	93.7	86.1	13.4	436.8	42.4	199.5	1087.5
OBZ-POSS	12.8	107.5	84.6	93.2	14.6	470.1	52.1	181.1	189.5

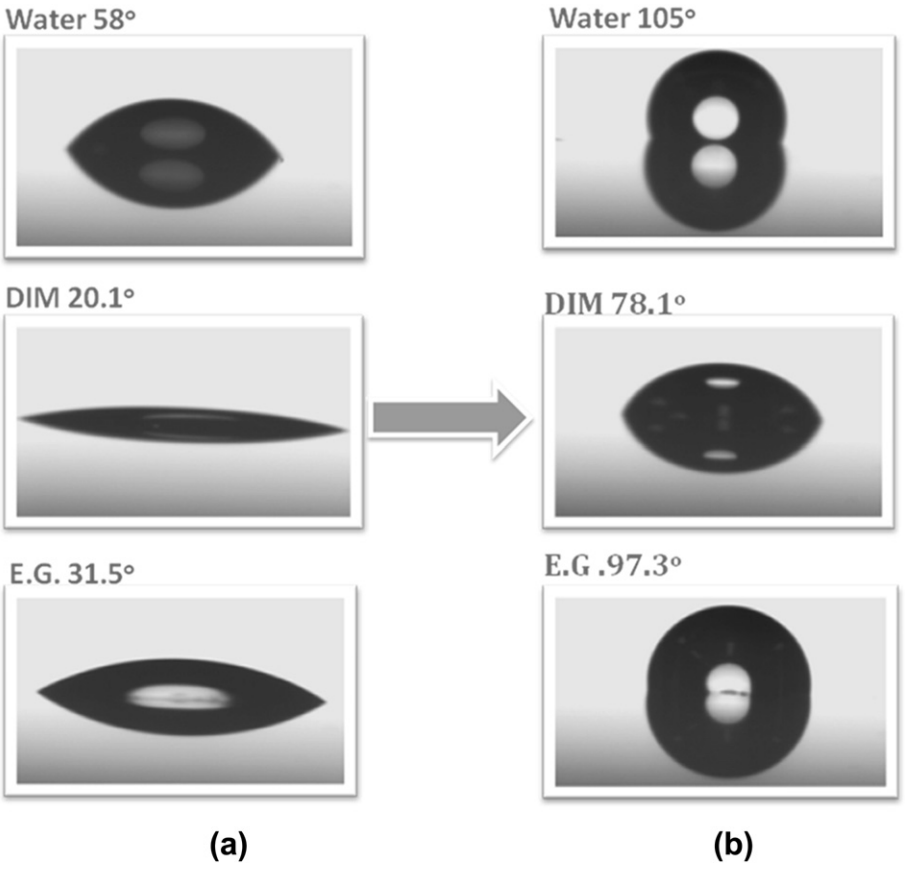

Fig. 10. The advancing contact angle for water, ethylene glycol (EG), and diiodomethane (DIM) of (a) poly(4-vinyl pyridine) thin film (b) modified with OBZ-POSS thin film.

Fig. 8 presents the FTIR spectra of pure OBZ-POSS after curing at 130 °C for various lengths of time. The characteristic absorption bands of the trisubstituted aromatic ring (1498 and 943 cm^{-1}) of OBZ-POSS disappeared during the early stages of curing (ca. 10–15 min). In addition, the absorption at 3135 cm^{-1}, corresponding to the stretching of the C=C bonds in the triazole structures, remained, implying that the triazole group did not react during thermal curing.

3.5. Thermal properties of OBZ-POSS

Fig. 9 gives the thermal stabilities under nitrogen of the polybenzoxazine/POSS nanocomposites. The curing condition used for OBZ-POSS composites was stirred for 2 h at room temperature and tipped out on the aluminum plate for 6 h in open air to dry and placed in an oven at 100 °C under vacuum for 2 h. The cast film was polymerized in a stepwise manner, at 140 and 160 °C for 3 h each and then at 200 °C for 4 h. The product was postcured at 220 and 240 °C for 30 min each. In a comparison of the thermal stabilities, we used 20 wt% weight loss temperature as a standard. An increase in the decomposition temperature (T_d) of the OBZ-POSS nanocomposite compared with P-pa and BA-m was observed. The difference in the decomposition temperature might be construed as an effect of creating the nanocomposite. In the nanocomposite material, thermal motion was restricted, thereby reducing the organic decomposition pathways. The inorganic component (POSS) provided additional heat capacity, thereby stabilizing the materials against thermal decomposition. Char yielding, another indicator of thermal stability, also increased upon increasing the POSS content of this hybrid material. The results indicated that the thermal stability of polybenzoxazines improved through network structures and the inorganic silsesquioxane.

Table 1 lists the surface advancing contact angles and surface energies, measured using the three testing liquids of BA-m, P-pa, and OBZ-POSS nanocomposites. Strikingly, the OBZ-POSS sample had a surface energy (14.6 mJ/m^2) lower than that of poly(tetrafluoroethylene) (PTFE) (22 mJ/m^2 as measured using the same method) [65]. Since we performed the thermal curing process of this OBZ-POSS nanocomposite at 120 °C, therefore, the spectra as shown in Fig. 6 could be used to modify many polymer substrates. Fig. 10 shows the advancing contact angles of water, ethylene glycol, and diiodomethane on the poly(4-vinyl pyridine) thin film before and after modification with OBZ-POSS; the advancing contact angles of the three test liquids all increased substantially. Moreover, this system also could modify many polymer substrates, such as poly(vinyl phenol) and poly(carbonate), that were thermally stable at or above 120 °C.

4. Conclusions

We have synthesized a novel octafunctionalized benzoxazine POSS (OBZ-POSS) from $OVBN_3$-POSS with P-pa via a click reaction. TGA analyses revealed that the decomposition temperatures of OBZ-POSS improved by incorporating POSS nanocomposites due to the POSS moieties that were distributed preferentially on the surface of the nanocomposite to provide a barrier, which could be identified by surface free energy analysis. The lower curing temperature of OBZ-POSS could be used to modify many polymer substrates, such as poly(4-vinyl pyridine), poly(vinyl phenol), and poly(carbonate), that are thermally stable at or above 120 °C.

Acknowledgment

This study was supported financially by the National Science Council, Taiwan, Republic of China, under contracts NSC97-2221-E-110-013-MY3, NSC98-2221-E-110-006 and NSC 98-2120-M-009-001.

References

[1] Riess G, Schwob JM, Guth G, Roche M, Lande B. In: Culbertson BM, McGrath JE, editors. Advances in polymer synthesis. New York: Plenum; 1985.
[2] Burke W. J Org Chem 1949;71:109.
[3] Takeichi T, Kawauchi T, Agag T. Polym J 2008;40:1121.
[4] Ishida H, Allen DJ. J Polym Sci Part B Polym Phys 1996;34:1019.
[5] Nair CPR. Prog Polym Sci 2004;29:401.
[6] Ghosh NN, Kiskan B, Yagci Y. Prog Polym Sci 2007;32:1344.
[7] Yagci Y, Kiskan B, Ghosh NN. J Polym Sci Part A Polym Chem 2009;47:5565.
[8] Wang CF, Su YC, Kuo SW, Huang CF, Sheen YC, Chang FC. Angew Chem Int Ed 2006;45:2248.
[9] Kuo SW, Wu YC, Wang CF, Jeong KU. J Phys Chem C 2009;113:20666.
[10] Wang CF, Chiou SF, Ko FH, Chen JK, Chou CT, Huang CF, et al. Langmuir 2007;23:5868.
[11] Ishida H, Allen DJ. Polymer 1996;39:4487.
[12] Ishida H, Lee YH. J Polym Sci Part B Polym Phys 2001;39:736.
[13] Ishida H, Lee YH. Polymer 2001;42:6971.
[14] Takeichi T, Agag T, Zeidam R. J Polym Sci Part A Polym Chem 2001;39:2633.
[15] Rimdusit S, Ishida H. Polymer 2000;41:7941.
[16] Takeichi T, Guo Y, Agag T. J Polym Sci Part A Polym Chem 2000;38:4165.
[17] Takeichi T, Guo Y. Polym J 2001;33:437.
[18] Su YC, Kuo SW, Xu HY, Chang FC. Polymer 2003;44:2187.
[19] Takeichi T, Guo Y, Rimdusit S. Polymer 2005;46:4909.
[20] Huang JM, Kuo SW, Lee YJ, Chang FC. J Polym Sci Polym Phys 2007;45:644.
[21] Agag T, Takeichi T. Polymer 2000;41:7083.
[22] Phirivawirut P, Magaraphan R, Ishida H. Mater Res Innovat 2001;4:187.
[23] Fu HK, Huang CF, Kuo SW, Lin HC, Yei DR, Chang FC. Macromol Rapid Commun 2008;29:1216.
[24] Kim HJ, Brunovska Z, Ishida H. Polymer 1999;40:1815.
[25] Chernykh A, Agag T, Ishida H. Polymer 2009;50:3153.
[26] Agag T, Takeichi T. Macromolecules 2001;34:7257.
[27] Agag T, Takeichi T. Macromolecules 2003;36:6010.
[28] Kiskan B, Yagci Y. Polymer 2004;49:2455.
[29] Kiskan B, Aydoan B, Yagci Y. J Polym Sci Part A Polym Chem 2009;47:804.
[30] Chernykh A, Agag T, Ishida H. Macromolecules 2009;42:5121.
[31] Kolb HC, Finn MG, Sharpless KB. Angew Chem Int Ed 2001;40:2004.
[32] Rostovtsev VV, Green LG, Fokin VV, Sharpless KB. Angew Chem Int Ed 2002;41:2596.
[33] Tornoe CW, Christensen C, Meldal M. J Org Chem 2002;67:3057.
[34] Ergin M, Kiskan B, Gacal B, Yagci Y. Macromolecules 2007;40:4724.
[35] Chemykh A, Agag T, Ishida H. Polymer 2009;50:382.
[36] Liao CS, Wu JS, Wang CF, Chang FC. Macromol Rapid Commun 2008;29:52.
[37] Velez-Herrera P, Ishida H. J Polym Sci Part A Polym Chem 2009;47:5871.
[38] Li GZ, Wang LC, Ni HL, Pittman CU. J Inorg Organomet Polym 2001;11:123.
[39] Phillips SH, Haddad TS, Tomczak SJ. Curr Opin Solid State Mater Sci 2004;8:21.
[40] Joshi M, Butola BS. J Macromol Sci Polym Rev 2004;C44:389.
[41] Mark JE. Acc Chem Res 2004;37:946.
[42] Pielichowaski K, Niuguna J, Janowski B, Pielichowski J. Adv Polym Sci 2006;201:225.
[43] Lickiss PD, Rataboul F. Adv Organmetal Chem 2008;57:1.
[44] Xu H, Kuo SW, Lee JS, Chang FC. Macromolecules 2002;35:8788.
[45] Kuo SW, Lee HF, Huang WJ, Jeong KU, Chang FC. Macromolecules 2009;42:1619.
[46] Kuo SW, Wu YC, Lu CH, Chang FC. J Polym Sci Polym Phys 2009;47:811.
[47] Huang CF, Kuo SW, Lin FJ, Huang WJ, Wang CF, Chen WY, et al. Macromolecules 2006;39:300.
[48] Sellinger A, Laine RM. Macromolecules 1996;29:2327.
[49] Lichtenhan JD, Otonari YA, Carr MJ. Macromolecules 1995;28:8435.
[50] Zheng L, Farris RJ. J Polym Sci Part A Polym Chem 2001;39:2920.
[51] Son S, Won J, Kim JJ, Jang YD, Kang YS, Kim SD. ACS Appl Mater Interfaces 2009;1:393.
[52] Haddad TS, Lichtenhan JD. Macromolecules 1996;29:7302.
[53] Subianto S, Mistry MK, Choudhury NR, Dutta NK, Knott R. ACS Appl Mater Interfaces 2009;1:1173.
[54] Chen Q, Xu R, Zhang J, Yu D. Macromol Rapid Commun 2005;26:1878.
[55] Liu Y, Zheng S. J Polym Sci Part A Polym Chem 2006;44:1168.
[56] Lee YJ, Huang JM, Kuo SW, Chen JK, Chang FC. Polymer 2004;46:2320.
[57] Xu HY, Kuo SW, Lee JS, Chang FC. Polymer 2002;43:5117.
[58] Ge Z, Wang D, Zhou Y, Liu H, Liu S. Macromolecules 2009;42:2903.
[59] Ervithayasuporn V, Wang X, Kawakami Y. Chem Commun 2009:5130.
[60] Zeng K, Zheng S. Macromol Chem Phys 2009;210:783.
[61] Lee YJ, Kuo SW, Huang CF, Chang FC. Polymer 2006;47:4378.
[62] Huang JM, Kuo SW, Huang HJ, Wang YX, Chen YT. J Appl Polym Sci 2009;111:628.
[63] Kim HD, Ishida H. J Phys Chem A 2002;106:3271.
[64] Xu HY, Kuo SW, Chang FC. Polym Bull 2002;48:469.
[65] Yoshimasa U, Takashi N. Langmuir 2005;21:2614.